

Unpaired Image Demoiréing Based on Cyclic Moiré Learning

Hyunkook Park[†], An Gia Vien[†], Yeong Jun Koh[‡], and Chul Lee[†]

[†]Department of Multimedia Engineering, Dongguk University, Seoul, Korea

E-mail: {hyunkook, viengiaan}@mme.dongguk.edu, chullee@dongguk.edu

[‡]Department of Computer Science and Engineering, Chungnam National University, Daejeon, Korea

E-mail: yjkoh@cnu.ac.kr

Abstract—We propose an end-to-end unsupervised learning approach to image demoiréing based on cyclic moiré learning. The proposed cyclic moiré learning consists of the moiré learning network and demoiréing network. The moiré learning network generates moiré images to construct a paired set of moiré and clean images. Then, the demoiréing network is trained using the generated paired dataset to remove moiré artifacts. Further, the moiré learning network and the demoiréing network are integrated together to be trained in an end-to-end manner. Experimental results demonstrate that the proposed algorithm outperforms state-of-the-art unsupervised image restoration algorithms.

I. INTRODUCTION

Despite recent significant advances in digital imaging technologies, undesired artifacts appear in captured images, degrading image quality, depending on capturing environments. For example, when we take pictures of screens, undesired colorful artifacts, called moiré artifacts, may appear in captured images. Moiré artifacts are disruptive colorful patterns with complex shapes and color variations. These moiré artifacts are caused by frequency aliasing between the camera's color filter array and the screen's subpixel layout. Extensive research has been made to remove moiré artifacts in screen-captured images. However, moiré artifact removal remains challenging, since moiré artifacts are diverse and spread over a wide range of regions in both spatial and frequency domains.

Early research on image demoiréing focused on the prior information of moiré artifacts. For example, Pekkukuksen and Altunbasak [1] and Menon and Calvagno [2] used multiscale color gradients of multiple directions during demosaicking. Yang *et al.* [3] removed moiré artifacts by dichotomizing a moiré image into a background layer and a moiré layer based on the assumption that moiré artifacts can be represented as a sparse matrix in the frequency domain. Yang *et al.* [4] further improved the decomposition-based demoiréing by exploiting the low-rank and sparse constraints on the texture and moiré images, respectively. However, since these model-based algorithms rely on the specific priors of the moiré artifacts, they may fail to effectively remove real-world moiré artifacts.

This work was supported in part by the National Research Foundation of Korea (NRF) grant funded by the Korea Government (MSIT) (No. NRF-2019R1A2C4069806) and in part by the Institute for Information & communications Technology Planning & Evaluation (IITP) grant funded by the Korea government (MSIT) (No.2019-0-01343, Training Key Talents in Industrial Convergence Security).

Recently, learning-based approaches using convolutional neural networks (CNNs) have achieved significant performance improvement in image demoiréing through learning from large-scale datasets. For example, in [5], [6], multiscale CNNs were employed for image demoiréing. He *et al.* [7] exploited the multiple prior information to consider various types of moiré patterns, including edge information and appearance attributes. Also, frequency information has been exploited in learning-based image demoiréing [8]–[10]. Zheng *et al.* [8] developed learnable multiscale bandpass filters to deal with the diversity of moiré artifacts in the frequency domain. Vien *et al.* [9], [10] proposed joint learning approaches to effectively exploit different characteristics of moiré artifacts in both spatial and frequency domains. However, the existing learning-based approaches are based on supervised learning, which requires large amounts of paired clean and moiré images. To address this limitation, Liu *et al.* [11] developed an unsupervised deep learning technique by employing a generative adversarial network (GAN) to handle real-world moiré images. However, it also used paired training data in the early training stage.

In this work, we develop an end-to-end image demoiréing algorithm using an unpaired set of clean and moiré images based on cyclic moiré learning. The cyclic moiré learning consists of two networks: *moiré learning network* and *demoiréing network*. The moiré learning network learns the distribution of moiré artifacts from unpaired dataset and generates a paired clean and moiré image set. The demoiréing network is trained with the generated paired dataset in a supervised manner. In addition, to improve the training efficiency, we propose a two-stage training scheme for each network. Experimental results show that the proposed algorithm provides higher demoiréing performance than the state-of-the-art unsupervised image restoration algorithms [12]–[14].

II. PROPOSED ALGORITHMS

We develop a learning-based end-to-end demoiréing algorithm using an unpaired clean and moiré image dataset. Fig. 1 shows the overall framework of the proposed algorithm. Suppose that we are given the sets of clean images $\{I_i^c\}_{i=1}^M$ and moiré images $\{I_i^m\}_{i=1}^N$. The proposed algorithm consists of two types of GANs. The first GAN in Fig. 1(a), called moiré learning network, degrades the clean images $\{I^c\}$ by

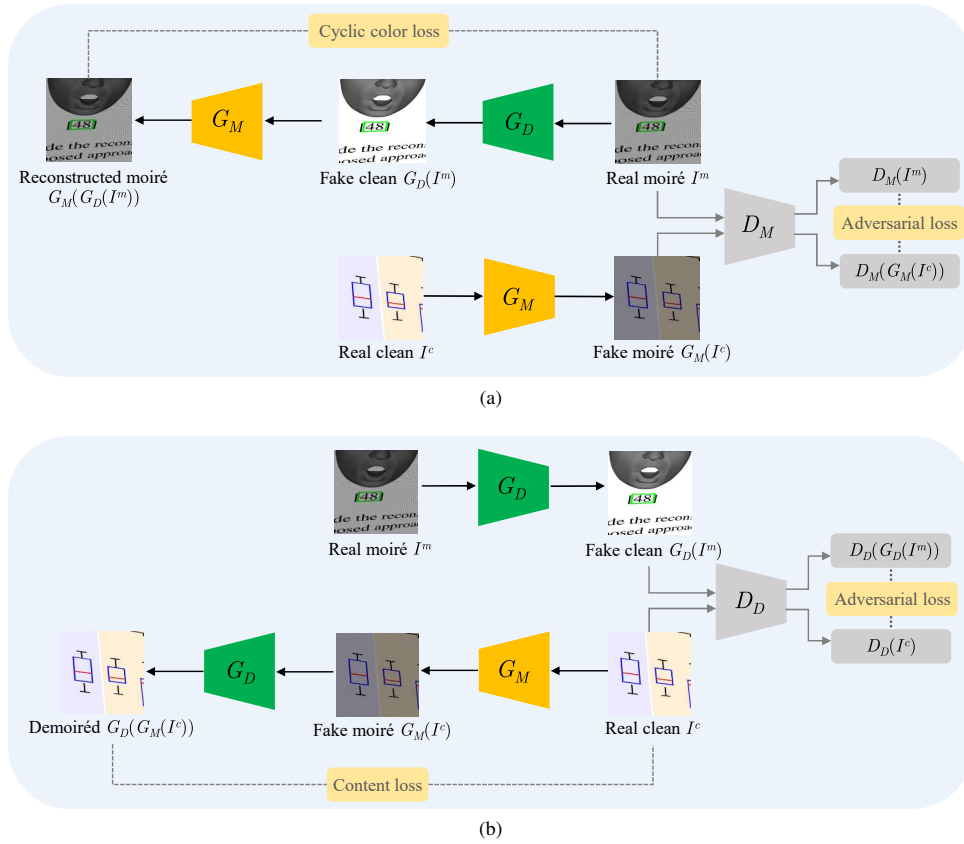


Fig. 1. Overview of the proposed unpaired demoiréing algorithm. (a) The moiré learning network learns to construct the pseudo pairs $\{I^c, G_M(I^c)\}$ given trained generator G_D , and (b) the demoiréing network is trained with the pseudo pairs $\{I^c, G_M(I^c)\}$ in a supervised manner with learned G_M .

adding moiré artifacts. The second GAN in Fig. 1(b), called demoiréing network, removes moiré artifacts in the moiré images $\{I^m\}$. Let G_M and G_D denote the generators to add moiré artifacts in clean images and remove moiré artifacts in moiré images, respectively. Similarly, D_M and D_D denote discriminators to discriminate between real moiré images $\{I^m\}$ and generated fake moiré images $\{G_M(I^c)\}$ and between demoiréed images $\{G_D(I^m)\}$ and clean images $\{I^c\}$, respectively. In other words, the moiré learning network constructs the pseudo pairs $\{I^c, G_M(I^c)\}$ given trained generator G_D , while the demoiréing network learns to remove moiré artifacts using the pseudo pairs $\{I^c, G_M(I^c)\}$ in a supervised manner with learned G_M . Let us describe each network subsequently.

A. Moiré Learning Network

As mentioned earlier, the moiré learning network in Fig. 1(a) generates fake moiré images $\{G_M(I^c)\}$ by learning the distribution of moiré artifacts in the real moiré images $\{I^m\}$. Thus, the moiré learning network constructs the pseudo pairs $\{I^c, G_M(I^c)\}$ of clean and moiré images, which will be used to train the demoiréing network.

It is well-known that training GANs may become unstable and needs tricks [15]. Thus, if the moiré learning network is trained with a single GAN, it cannot guarantee that the generated fake moiré images are mapped to desired real moiré

images. To address this issue and make the training of the moiré learning network stable, we employ cyclic color consistency [16], which enforces similarity of the reconstructed image to its origin. Specifically, the generator G_M is learned to yield reconstructed moiré images $\{G_M(G_D(I^m))\}$ that are similar to the moiré images $\{I^m\}$. This cyclic color consistency makes the moiré learning network generate more realistic artifacts while preserving the original clean image’s information.

Fig. 2 shows the detailed architecture of generator G_M in Fig. 1. Moiré images contain both moiré patterns and color degradation, thus generator G_M should be capable of generating images with both moiré patterns and color degradation from clean images. To this end, we use two generators, G_{M1} and G_{M2} . The first generates color degradation, and the second generates moiré patterns. In addition, the proposed moiré learning network is based on the conditional generative adversarial network (cGAN) [17]. Specifically, we use a clean image I^c as conditional information for cGAN, which enables the network to generate complex moiré artifacts by exploiting the correlation between generated fake moiré images and real clean images.

Architecture of the generators: We design a U-Net-like structure [18] that takes a real clean image and random noise as

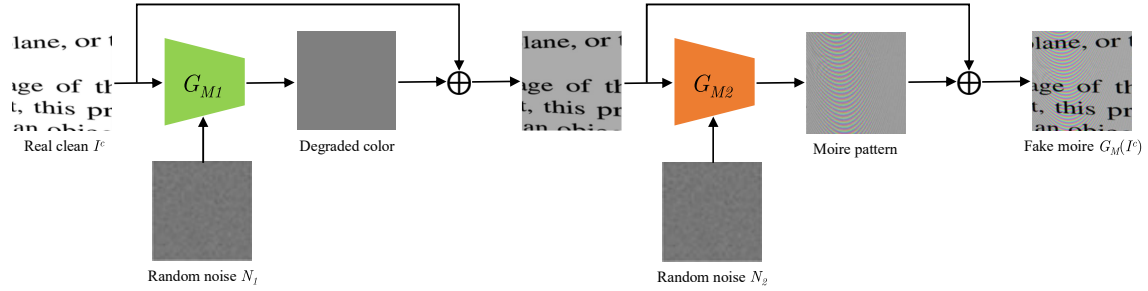


Fig. 2. Architecture of generator G_M that adds moiré artifacts in clean images $\{I^c\}$ to synthesize fake moiré images $\{G_M(I^c)\}$. The generator G_M consists of two generators: G_{M1} generates degraded colors, while G_{M2} generates moiré patterns.

input. The generator consists of an encoder, a decoder, and skip connections at each scale. The encoder has four scales, each of which consists of two convolutional layers with a kernel of 3×3 and a stride of 1 and a convolutional layer with a kernel of 2×2 and a stride of 2. Each convolutional layer is followed by a rectified linear unit (ReLU) layer. The decoder consists of upsampling operators and two convolutional layers with a kernel of 3×3 and a stride of 1 followed by a ReLU layer. At the final scale, a 1×1 convolutional layer is used to obtain the generated image.

Architecture of the discriminator: We employ the discriminator network of DCGAN [19] as the baseline. To improve the performance of the discriminator, we remove the batch normalization layers and add two more convolutional layers with ReLU, which increases the receptive field of the network. Furthermore, to make the discriminator focus more on moiré patterns, in addition to an image, we use high frequency components in the image as input to the discriminator. The high frequency components are obtained by applying a low-pass filter to the image and then subtracting the low-pass filtered image from the input image.

B. Demoiréing Network

Once the moiré learning network constructs the pseudo pairs $\{I^c, G_M(I^c)\}$, the demoiréing network is trained to remove moiré artifacts in a supervised manner using the learned G_M as shown in Fig. 1(b). The overall structure of the demoiréing network is similar to that of the moiré learning network. The main difference is that the cyclic color consistency is computed between I^c and $G_M(I^c)$, which we call the content loss.

Architecture of the generator: The demoiréing network architecture is based on U-Net [18] with four scales. We employ residual blocks (RBs) for exploiting complex moiré patterns by learning features at multiple levels of abstraction. Each level of the encoder consists of a convolutional layer with a kernel of 3×3 and a stride of 1, three RBs, and a convolutional layer with a kernel of 2×2 and a stride of 2 for downsampling. Each convolutional layer is followed by a ReLU layer. Then, deeper moiré features are extracted using three RBs. The architecture of the decoder is the same as that of the generator in the moiré learning network.

C. Loss Functions

Moiré learning network: To train the moiré learning network, we define the moiré learning loss \mathcal{L}_M as

$$\mathcal{L}_M = \mathcal{L}_{G_M} + \lambda_M \mathcal{L}_{\text{cycle}} \quad (1)$$

where \mathcal{L}_{G_M} and $\mathcal{L}_{\text{cycle}}$ are the generator loss and the cyclic color consistency loss, respectively. Also, the parameter λ_M controls the relative impact between the two losses.

For training the generator G_M and discriminator D_M , we employ the least squares generative adversarial network (LSGAN) [20] to define loss functions. Specifically, we define the generator loss \mathcal{L}_{G_M} and discriminator loss \mathcal{L}_{D_M} , respectively, as

$$\mathcal{L}_{G_M} = \mathbb{E}_{I^c \sim p(I^c)} [(D_M(G_M(I^c)) - 1)^2] \quad (2)$$

$$\mathcal{L}_{D_M} = \mathbb{E}_{I^m \sim p(I^m)} [(D_M(I^m) - 1)^2] + \mathbb{E}_{I^c \sim p(I^c)} [D_M(G_M(I^c))^2]. \quad (3)$$

Next, we define the cyclic color consistency loss $\mathcal{L}_{\text{cycle}}$ for the moiré learning network as the L_1 norm between the reconstructed moiré image and the original moiré image as

$$\mathcal{L}_{\text{cycle}} = \mathbb{E}_{I^m \sim p(I^m)} [\|G_M(G_D(I^m)) - I^m\|_1]. \quad (4)$$

Demoiréing network: We define the demoiréing loss \mathcal{L}_D as the sum of the generator loss \mathcal{L}_{G_D} and the content loss $\mathcal{L}_{\text{content}}$ between I^c and its cyclically generated version, given by

$$\mathcal{L}_D = \mathcal{L}_{G_D} + \lambda_D \mathcal{L}_{\text{content}} \quad (5)$$

where λ_D is a trade-off parameter between the two losses.

The generator and discriminator losses for G_D and D_D , respectively, are defined as

$$\mathcal{L}_{G_D} = \mathbb{E}_{I^m \sim p(I^m)} [(D_D(G_D(I^m)) - 1)^2] \quad (6)$$

$$\mathcal{L}_{D_D} = \mathbb{E}_{I^c \sim p(I^c)} [(D_D(I^c) - 1)^2] + \mathbb{E}_{I^m \sim p(I^m)} [D_D(G_D(I^m))^2]. \quad (7)$$

Finally, we compute the content loss for the demoiréing network as the sum of the L_1 loss and advanced Sobel loss (ASL) [8], given by

$$\mathcal{L}_{\text{content}} = \mathbb{E}_{I^c \sim p(I^c)} [\|G_D(G_M(I^c)) - I^c\|_1] + \lambda_c \mathbb{E}_{I^c \sim p(I^c)} \left[\sum_{i=1}^4 \|S_i(G_D(G_M(I^c))) - S_i(I^c)\|_1 \right] \quad (8)$$

TABLE I
QUANTITATIVE COMPARISON OF THE PROPOSED ALGORITHM WITH CYCLEGAN [12], CWR [13], AND UID-NET [14].

	CycleGAN [12]	CWR [13]	UID-Net [14]	Proposed
PSNR	20.96	23.86	24.17	26.23
SSIM	0.8659	0.9276	0.8921	0.9504

where λ_c is a trade-off parameter between the L_1 loss and ASL, and $S_i(\cdot)$ denotes the edge map obtained by the i th filter in the Sobel filtering among the horizontal, vertical, and two diagonal filters.

III. EXPERIMENTAL RESULTS

A. Dataset

We evaluate the performance of the proposed algorithm on the LCDMoire dataset [21]. The LCDMoire dataset contains 10,100 synthetic moiré and clean image pairs, which are composed of 10,000 training pairs and 100 validation pairs. To construct the unpaired moiré dataset, we divide 10,000 training pairs into two groups, and then pick 5,000 moiré images from the first group and 5,000 clean images from the second group. We use the unpaired moiré dataset for training the proposed networks and the 100 validation pairs for the test.

B. Implementation Details

We train the proposed networks using the AdamW optimizer [22] with a learning rate of 10^{-4} , $\beta_1 = 0.5$, and $\beta_2 = 0.999$. The batch size is fixed to 16. The training is iterated for 150 epochs and takes about 12 hours using an Nvidia GeForce RTX 2080 Ti GPU. During training, we randomly crop patches of size 64×64 and shuffle moiré and clean patches for each epoch. In the test, the test images of the original resolution (1024×1024) are used. The weight parameters λ_M in (1), λ_D in (5), and λ_c in (8) are set to 10, 10, and 0.5, respectively. Also, the kernel size for low-pass filtering is 3×3 .

C. Quantitative and Qualitative Evaluation

To the best of our knowledge, this is the first attempt for unpaired image demoiréing. Thus, by considering unpaired image demoiréing as an image-to-image translation task, we compare the proposed algorithm with the existing unpaired image-to-image translation algorithms CycleGAN [12] and CWR [13]. Also, we compare the proposed algorithm with the unsupervised image denoising algorithm UID-Net [14].

For quantitative assessment, we employ the PSNR and the structural similarity index (SSIM) [23] metrics. Table I shows the average PSNR and SSIM scores over all images on the validation set in LCDMoire. The proposed algorithm outperforms all other unsupervised algorithms, providing the higher PSNR score than CycleGAN, CWR, and UID-Net with margins 5.27, 2.37, and 2.06 dB, respectively. The proposed algorithm also provides the best demoiréing performance in terms of SSIM. This indicates that the cyclic moiré learning is effective for unpaired image demoiréing.

TABLE II
IMPACTS OF THE CYCLIC COLOR CONSISTENCY AND DUAL GENERATOR.

Cycle	G_{M2}	PSNR	SSIM
		23.91	0.9272
	✓	25.29	0.9368
✓		25.89	0.9414
✓	✓	26.23	0.9504

Fig. 3 compares demoiréing results qualitatively. The existing algorithms fail to remove complex moiré patterns and to restore color degradation. For example, in the first row in Fig. 3(c), CycleGAN loses the original colors in the yellow and green rectangles. Also, in the second and fourth rows, CycleGAN fails to remove complex moiré patterns. In Fig. 3(d), CWR [13] removes moiré artifacts faithfully, but it provides brightness changes, as shown in the second and third rows. UID-Net [14] in Fig. 3(e) preserves information of the original images, but it fails to remove complex moiré patterns as shown in the first and fourth rows and to restore color intensity faithfully. On the contrary, the proposed algorithm effectively removes moiré artifacts while reconstructing the color information faithfully.

Finally, to demonstrate the effectiveness of the cyclic color consistency and a dual generator in the moiré learning network, we conducted several ablation experiments. In Table II, we observe that the performance is degraded severely without both the cyclic color consistency and the second generator. This indicates that both the cycle consistency and the second generator are essential components of the proposed algorithm for unpaired image demoiréing.

IV. CONCLUSIONS

We proposed an end-to-end unsupervised demoiréing algorithm using an unpaired training dataset based on cyclic moiré learning. The proposed network consists of the moiré learning network and demoiréing network. The moiré learning network constructs the paired dataset from an unpaired dataset, whereas the demoiréing network is trained to remove moiré artifacts in a supervised manner. Also, we reinforced the cyclic color consistency, so that the moiré learning network generates moiré-looking artifacts while preserving information of the original clean image. Experimental results demonstrated that the proposed algorithm outperforms state-of-the-art unsupervised image restoration algorithms.

REFERENCES

- [1] I. Pekkucuksen and Y. Altunbasak, "Multiscale gradients-based color filter array interpolation," *IEEE Trans. Image Process.*, vol. 22, no. 1, pp. 157–165, Jan. 2013.
- [2] D. Menon and G. Calvagno, "Color image demosaicking: An overview," *Signal Process.: Image Commun.*, vol. 26, no. 8, pp. 518–533, Oct. 2011.
- [3] J. Yang, X. Zhang, C. Cai, and K. Li, "Demoiréing for screen-shot images with multi-channel layer decomposition," in *Proc. IEEE Vis. Commun. Image Process.*, Dec. 2017, pp. 1–4.
- [4] J. Yang, F. Liu, H. Yue, X. Fu, C. Hou, and F. Wu, "Textured image demoiréing via signal decomposition and guided filtering," *IEEE Trans. Image Process.*, vol. 26, no. 7, pp. 3528–3541, Dec. 2017.

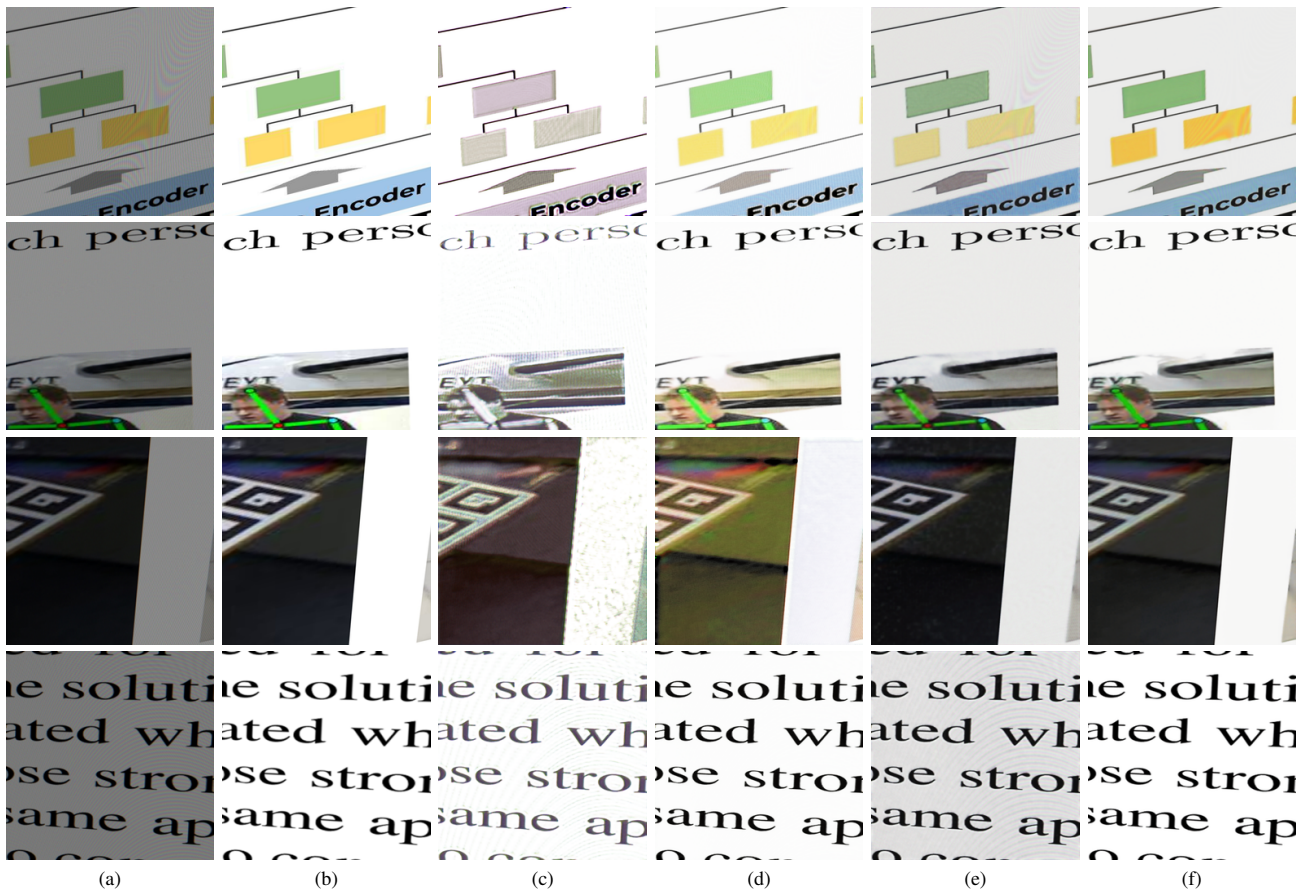


Fig. 3. Qualitative comparison of demoiréing results for the validation set in the LCDMoiré dataset [21]: (a) moiré image, (b) ground-truth, and outputs of (c) CycleGAN [12], (d) CWR [13], (e) UID-Net [14], and (f) the proposed algorithm.

[5] Y. Sun, Y. Yu, and W. Wang, "Moiré photo restoration using multiresolution convolutional neural networks," *IEEE Trans. Image Process.*, vol. 27, no. 8, pp. 4160–4172, Aug. 2018.

[6] X. Cheng, Z. Fu, and J. Yang, "Multi-scale dynamic feature encoding network for image demoiréing," in *Proc. IEEE Int. Conf. Comput. Vis. Workshops*, Oct. 2019, pp. 3486–3493.

[7] B. He, C. Wang, B. Shi, and L. Duan, "Mop moiré patterns using MopNet," in *Proc. IEEE Int. Conf. Comput. Vis.*, Oct. 2019, pp. 2424–2432.

[8] B. Zheng, S. Yuan, G. Slabaugh, and A. Leonardis, "Image demoiréing with learnable bandpass filters," in *Proc. IEEE Conf. Comput. Vis. Pattern Recognit.*, Jun. 2020, pp. 3636–3645.

[9] A. G. Vien, H. Park, and C. Lee, "Dual-domain deep convolutional neural networks for image demoiréing," in *Proc. IEEE Conf. Comput. Vis. Pattern Recognit. Workshops*, Jun. 2020, pp. 1934–1942.

[10] A. G. Vien, H. Park, and C. Lee, "Moiré artifacts removal in screenshot images via multiple domain learning," in *Proc. Asia Pac. Signal Inf. Process. Assoc. Annu. Summit Conf.*, Dec. 2020, pp. 1268–1273.

[11] B. Liu, X. Shu, and X. Wu, "Demoiréing of camera-captured screen images using deep convolutional neural network," *arXiv preprint arXiv:1804.03809*, 2018.

[12] J.-Y. Zhu, T. Park, P. Isola, and A. A. Efros, "Unpaired image-to-image translation using cycle-consistent adversarial networks," in *Proc. IEEE Int. Conf. Comput. Vis.*, Oct. 2017, pp. 2223–2232.

[13] J. Han, M. Shoebiy, T. Malthus, E. Botha, J. Anstee, S. Anwar, R. Wei, L. Petersson, and M. A. Armin, "Single underwater image restoration by contrastive learning," in *Proc. IEEE Int. Geosci. Remote Sens. Symp.*, Jul. 2021.

[14] Z. Hong, X. Fan, T. Jiang, and J. Feng, "End-to-end unpaired image denoising with conditional adversarial networks," in *Proc. AAAI Conf. Artif. Intell.*, Apr. 2020, pp. 4140–4149.

[15] J. Chen, J. Chen, H. Chao, and M. Yang, "Image blind denoising with generative adversarial network based noise modeling," in *Proc. IEEE Conf. Comput. Vis. Pattern Recognit.*, Jun. 2018, pp. 3155–3164.

[16] H.-U. Kim, Y. J. Koh, and C.-S. Kim, "Global and local enhancement networks for paired and unpaired image enhancement," in *Proc. European Conf. Comput. Vis.*, Aug. 2020, pp. 339–354.

[17] M. Mirza and S. Osindero, "Conditional generative adversarial nets," *arXiv preprint arXiv:1411.1784*, 2014.

[18] O. Ronneberger, P. Fischer, and T. Brox, "U-Net: Convolutional networks for biomedical image segmentation," in *Proc. Med. Imag. Comput. Computer-Assisted Intervention*, Nov. 2015, pp. 234–241.

[19] A. Radford, L. Metz, and S. Chintala, "Unsupervised representation learning with deep convolutional generative adversarial networks," in *Proc. Int. Conf. Learn. Represent.*, May 2016, pp. 1–16.

[20] X. Mao, Q. Li, H. Xie, R. Y. K. Lau, Z. Wang, and S. P. Smolley, "Least squares generative adversarial networks," in *Proc. IEEE Int. Conf. Comput. Vis.*, Oct. 2017, pp. 2794–2802.

[21] S. Yuan, R. Timofte, G. Slabaugh, and A. Leonardis, "AIM 2019 challenge on image demoiréing: Dataset and study," in *Proc. IEEE Int. Conf. Comput. Vis. Workshops*, Oct. 2019, pp. 3526–3533.

[22] I. Loshchilov and F. Hutter, "Decoupled weight decay regularization," in *Proc. Int. Conf. Learn. Represent.*, May 2019.

[23] Z. Wang, A. C. Bovik, H. R. Sheikh, and E. P. Simoncelli, "Image quality assessment: From error visibility to structural similarity," *IEEE Trans. Image Process.*, vol. 13, no. 4, pp. 600–612, Apr. 2004.